Bull. Disas. Prev. Res. Inst., Kyoto Univ., Vol. 36, Parts 3, 4, No. 320, December, 1986 

# A Numerical Study of Mantle Tectonic Flow as Relevant to the Cenozoic Structural Development of the East Asiatic Transition Zone

By Keiichi NISHIMURA

(Manuscript received August 26, 1986)

**Abstract**

Based on an examination of historical sequence of the Cenozoic events in the East Asiatic transition zone, it is assumed that, at some stage of the Early Cenozoic, there was a significant difference in the temperature of the upper mantle between the two sides of the Japanese Islands, higher on the side under the Japan Sea and lower on the side under the northwestern Pacific Ocean. The mechanical aspect of mantle tectonic flow which could be generated as a result of this difference is numerically investigated with the use of the SOR method in combination with the MAC method. The basic features of fluid flow observed from the calculated result have significant implications with regard to the Cenozoic structural development of the East Asiatic transition zone, in support of the proposition that the density-driven differential mantle flow played a prominent role in the development of the present-day structure of the transition zone.

## 1. Introduction

An understanding of role and mechanism of mantle tectonic flow is of great importance in the study of structural development of the transition zone from the East Asiatic continent to the Pacific Ocean. The fundamental structural elements that constitute the present-day feature of the transition zone are marginal basin, island arc, deep-sea trench and the seismofocal Benioff zone. Although a few investigators regard the Japan Sea as a remnant of old ocean[1], many others consider that the present-day structure of the transition zone has been formed during the course of the late Cenozoic time. The latter point of view is supported by petrological evidence indicating that the Japan Sea appeared in the Neogene, as will be seen later in this paper.

It should be noted, however, that there is a wide divergence of opinion as to the role and mechanism of mantle tectonic flow in relevance to the Cenozoic evolution of the transition zone.

As is well known, most adherents of plate tectonics accept the schematic diagram according to which the generation of marginal basin is associated with the thermo-mechanical effects of tectonic flow induced in the "back-arc" mantle by the subduction of oceanic plate[2)~5)]. The same mechanism is also considered to be responsible for the formation of the mantle wedge, that is, the anomalously heated portion of upper mantle situated beneath the inner side of an island arc. It is true that plate

tectonics does not consider that the generation of all the marginal basins can be explained by one and the same mechanism, but the Japan Sea is considered to be one of those basins which were generated in accordance with the above diagram. What is important to note is that, in this diagram, the heating of the upper mantle under marginal basin is considered to be a result of subduction of oceanic plate; in the case of the Japan Sea, a result of westward subduction of the Pacific Plate.

On the other hand, the tectonic flow in the transition zone has been treated in a quite different way by those who argue against the subduction of oceanic plate. Various diagrams have been proposed[6)~9)]. A brief review of these diagrams shows that, while the concrete features of tectonic flow differ from diagram to diagram, there is a common feature wherein the generation of island arc—trench system and the Benioff zone is associated with relative movements in the mantle. Here we refer to the most comprehensive diagram proposed by Beloussov[9)]. In this diagram, the mantle tectonic flow is supposed to be caused by the density difference between the two sides of island arc, lower on the side under the marginal basin and higher on the side beneath and beyond the deep-sea trench. The density difference, in its turn, is supposed to be produced by the difference in the temperature of the upper mantle. The basic feature of the tectonic flow is visualized as follows: the mantle with lower density under the marginal basin would flow over the denser mantle beneath and beyond the deep-sea trench, and accordingly the denser mantle would flow under the mantle with lower density. What makes a decided contranst with the diagram of plate tectonics is that this diagram assumes that, before the formation of the present-day structure of the island arc—trench system, there was already a significant difference in the temperature of the upper mantle between the two sides of the island arc.

Accordingly, the difference in opinion is mainly concerned with the genetic relationship among the structural elements of the transition zone.

The main purpose of this paper is to numerically investigate the basic features of mantle tectonic flow which could be relevant to the Cenozoic evolution of the East Asiatic transition zone. For this purpose, it is necessary to assume a schematic model representing the deep-seated mantle condition under the transition zone which prevailed at some stage of the Early Cenozoic. However, the above consideration shows that there is a need, prior to numerical modelling, to discuss the problem of the historical sequence of Cenozoic events that took place in the East Asiatic transition zone. Thus this problem will be first considered by refering to some recent papers.

## 2. The Historical Sequence of the Cenozoic Events in the East Asiatic Transition Zone

In his previous paper[10)], the present writer has already examined the temporal and spatial characteristics of the Meso-Cenozoic tectonomagmatic activity that manifested itself in the vast area of East Asia, including the inner part of the East Asiatic continent as well as the transition zone. Taking into account the characteristic

feature that the most intensive activity migrated gradually from the inner part of the continent to its marginal part during the Mesozoic to Early Cenozoic time, it was suggested that the late Cenozoic activity in the East Asiatic transition zone was manifested as the continuation of this migration and was possibly associated with the corresponding eastward migration of the most heated portion of upper mantle.

This suggestion finds support in new results of a petrological study of volcanic rocks from the Japan Sea; quite recently, Florova and Konovalov[11] have shown that

(1) The volcanic activity within the region of the Japan Sea began more than 55 million years ago in the Early Paleogene. It started with the subaerial eruption of dacite, rhyolite and andesite magmas and partly of andesite-basalt magma. Since the middle Miocene, it changed to the subaqueous eruption mainly of basalt magma.

(2) There is a general trend that the volcanic activity began and ended earlier in the northwestern part of the Japan Sea than in its southeastern part. This can be attributed, in their opinion, to the eastward migration of the magma-generating sources in the upper mantle.

(3) The chemical composition of the volcanic rocks was characterized by the so-called "antidromal" change; namely, the volcanic rocks issued in the Neogene became more basic than those issued in the Paleogene.

These results have a significant implication with regard to the problem of the historical sequence of the Cenozoic events in the East Asiatic transition zone. The change in the character of volcanic eruption from subaerial to subaqueous(1) implies that the Japan Sea is not a remnant of old ocean, but is of secondary origin. It appeared in the Neogene(probably, in the middle Miocene). This is in agreement with the conclusion reached by Kaneoka[12], who investigated the radiometric ages of volcanic rocks dredged mostly from the southeastern half of the Japan Sea. It should be emphasized, however, that the finding of the Early Paleogene volcanic rocks, for example, andesites from the Yamato Bank dated to be 68.1 Ma[11], indicates that the upper mantle under the Japan Sea was already heated in the Early Paleogene. It is obvious that this heating preceded the Neogene to Quaternary activities, such as the Green-tuff and the Island-arc Disturbances, with which many geologists associate the formation of the modern structure of the Japanese Islands[13]. The temporal and spatial characteristics(2) of the Cenozoic volcanism in the Japan Sea seems to be in accord with those of the Mesozoic to Early Cenozoic acivity mentioned above. In addition, the "antidromal" change in the chemical composition of volcanic rocks(3) is similar to the corresponding change that characterized the Meso-Cenozoic magmatism over the East Asiatic continent, as pointed out in the previous paper[10]. Accordingly, the above results of the petrological study of volcanic rocks from the Japan Sea seem to favor the above-mentioned supposition of the present writer that the Cenozoic activity in the transition zone was manifested as the continuation of the Mesozoic to Early Cenozoic tectonomagmatic activity in the East Asiatic continent.

In contrast, according to the widely accepted diagram of plate tectonics the appearance of the Japan Sea is associated with the thermo-mechanical effects of the westward subduction of the Pacific Plate that started about 40 to 45 million years ago[14]; the convective flow in the "back-arc" mantle induced by the subduction played the leading role in the formation of the Japan Sea. This diagram appears, at a first glance, to plausibly explain the historical sequence of the Cenozoic events in the East Asiatic transition zone. However, it should be emphasized that the Early Paleogene volcanism mentioned above remains unexplained, because it started much earlier than the beginning of the westward subduction of the Pacific Plate. It is true that some adherents of plate tectonics consider that the westward subduction of the Pacific Plate was preceded by the northward(or northwestward) subduction of the Pacific and the Kula Plates[15], but no satisfactory explanation has yet been provided as to the reason why the Japan Sea was not formed as a result of this subduction which involved, in their opinion, even the active oceanic ridges. In this connection, it is interesting to note an important question about the feasibility of the current diagram of plate tectonics, which has been recently propounded by the petrological study of basaltic rocks from the inner part of the northeast Japan. Based on experimental study, Tatsumi et al.[16] have asserted that the temperature within the mantle wedge should be higher than 1,400°C. This temperature evidently is much higher than any theoretical value so far calculated based on the above-mentioned diagram of plate tectonics. Thus, the question is whether it is possible to explain such extremely high temperature in the framework of the current diagram of plate tectonics. An attempt to positively answer this question was made by Honda[17]. He carried out numerical calculations of temperature distribution in the mantle wedge and then concluded that the high temperature suggested by Tatsumi et al. can be explained by assuming that the upper mantle under the Japan Sea was already heated up to 1,400 °C at the depth shallower than 100 km. In order for this explanation to be accepted, it is necessary to assume that the upper mantle under the Japan Sea was heated independently of(and, possibly, prior to) the westward subduction of the Pacific Plate. This means as a logical consequence that the above-mentioned diagram of plate tectonics should be significantly modified in order to meet the requirement put forth by the petrological considerations. In fact, Miyashiro[18] has recently suggested an idea that the upper mantle under marginal basin was heated independently of the subduction of oceanic plate. Taylor and Karner[19] also have argued that the temporal and spatial distribution of marginal basins cannot be explained by those hypotheses that attribute the generation of marginal basins to plate subduction. This means that, even in the opinion of supporters of plate tectonics, the subducting plate begins to lose its important function as a causal factor of formation of marginal basins.

Accordingly, it seems possible to conclude from the above consideration that the historical sequence of the Cenozoic events in the East Asiatic transition zone supports the above-mentioned Beloussov's opinion about the genetic relationship among the structural elements of the transition zone. This means that the current diagram of

the plate tectonics, in which the subducting plate plays an important role as a causal factor of heating of the "back-arc" mantle, hardly can serve as a basis for numerical modelling of tectonic flow in the transition zone. Thus, in the following modelling, it will be assumed that the upper mantle under the Japan Sea was already heated in the Early Cenozoic as a result of the eastward migration of the most intensive tectonomagmatic activity from the inner part of the East Asiatic Continent to its marginal part, and special attention will be confined to the problem of actual possibility of the Beloussov's diagram, according to which the density-driven differential flows in the upper mantle played a prominent role in the formation of the present-day structure of the transition zone.

## 3. Numerical Modelling of Tectonic Flow in the Transition Zone

### (1) Initial condition

It is assumed that, at some stage of the Early Cenozoic, the upper mantle under the Japan Sea was significantly heated and, on the other hand, the upper mantle under the northwestern Pacific was already cooled. The latter assumption is made on the basis of the old age of the ocean floor and the low values of surface heat flow observed in the northwestern part of the Pacific ocean. Thus, as an initial condition, it is assumed that there was a significant difference in the temperature of the upper mantle under the East Asiatic transition zone.

In this connection, it is interesting to note that a similar assumption was already made by Shimazu and Kono[20] in their calculation of mantle convection. They showed that relative movements would be generated in the mantle. But, unfortunately, the significance of their result was obscured by the advent of plate tectonics which asserts that the heating of the "back-arc" mantle should be ascribed to the effect of plate subduction. It is noteworthy that the basic feature of tectonic flow visualized in the diagram of Beloussov is concordant with that of the relative movements shown by Shimazu and Kono. Although an extention of their method of calculation for more realistic models including several different fluids is desirable, great mathematical difficulty is encountered in combining the momentum equation with the energy equation; the two equations cannot be combined with each other by a single equation of state. Thus, the following consideration is confined to the mechanical aspect of tectonic flows which could be generated in the mantle consisting of several different fluids.

The enclosure shown in **Fig. 1** represents the initial state. It consists of five Newtonian, incompressible, viscous fluids. The fluid(1) stands for the lithosphere, the fluids(2) and (3) for the asthenosphere and the fluid(4) for the mesosphere. The fluid(0) with very low density and viscosity is inserted in order that the upper surface of the lithosphere behaves approximately as a free surface. The asthenosphere is divided into two different fluids, the fluid(2) with lower density and viscosity and the fluid(3) with higher density and viscosity. Thus, the left side of the

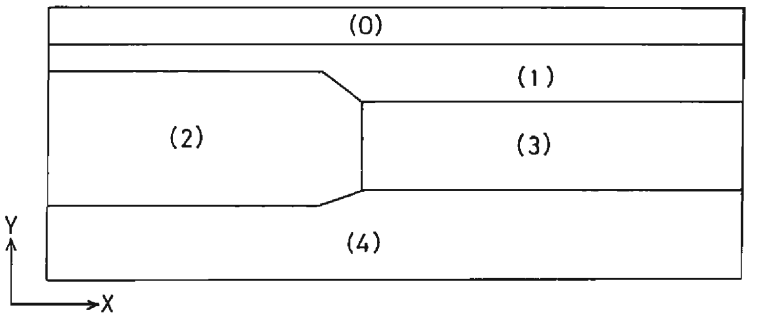


Fig. 1 Initial state for numerical calculation, schematically representing the deep-seated mantle condition at some stage of the Early Cenozoic.

enclosure composed of thin lithosphere and thick asthenosphere represents the anomalously heated mantle under the Japan Sea, and the right side composed of thick lithosphere and thin asthenosphere represents the cool mantle under the northwest Pacific. Although such a model is artificial, it is believed that it corresponds to the above-mentioned situation that, at some stage of the Early Cenozoic, there was a significant difference in the temperature of the upper mantle between the two sides of the Japanese Islands. In fact, this model conforms to the generalized scheme of Rodnikov and Vadkovsky[8] which was proposed based on detailed investigation of the deep-seated structure of the transition zone[21].

### (2) Basic Equation and Boundary Conditions

In general, there are three methods of numerical solution of the Navier-Stokes equation describing the motion of viscous fluids. The first one is to directly use the "primitive" variables, i.e. the velocity and the pressure. The original MAC method proposed by Harlow and Welch[22] is the premier example of this type of solution. The second and most popular method is the vorticity—stream function approach. In this method the pressure is eliminated by cross-differentiating the momemtum equations to yield two Poisson equations for the vorticity transport and for the stream function. The Poisson equations are separable if the viscosity is constant. The third method is to use the "generalized biharmonic equation" derived by eliminating the pressure and substituting the derivatives of stream function for the vorticity. In this paper, the third method is utilized, because this approach is more suitable for a variable viscosity problem and because there is no need to obtain the values of the pressure or the vorticity. The following derivation of the generalized biharmonic equation is due to Andrews[23], who first proposed this method.

The tectonic flow in the earth is so slow that the effect of intertia can be neglected and, therefore, the equation of motion can be expressed as the balance of stress, pressure and gravity terms. With respect to the coordinate system shown in **Fig. 1**, the equation of motion is expressed by the following two equations:

$$\left.\begin{aligned}&\frac{\partial \tau_{xx}}{\partial x}+\frac{\partial \tau_{xy}}{\partial y}-\frac{\partial P}{\partial x}=0\\&\frac{\partial \tau_{xy}}{\partial x}+\frac{\partial \tau_{yy}}{\partial y}-\frac{\partial P}{\partial y}-\rho g=0\end{aligned}\right\} \quad \cdots\cdots(1)$$

where $P$, $\rho$ and $g$ are pressure, density of the fluids and the gravitational acceleration, respectively, and $\tau_{xx}$, $\tau_{yy}$ and $\tau_{xy}$ are the stress components. Since the fluids are incompressible, the equation of continuity is reduced to:

$$\frac{\partial u}{\partial x}+\frac{\partial v}{\partial y}=0 \quad \cdots\cdots(2)$$

and then the stress components are expressed by

$$\left.\begin{aligned}&\tau_{xx}=-\tau_{yy}=2\eta\frac{\partial u}{\partial x}\\&\tau_{xy}=\eta\left(\frac{\partial u}{\partial y}+\frac{\partial v}{\partial x}\right)\end{aligned}\right\} \quad \cdots\cdots(3)$$

where $\eta$ is viscosity and $u$ and $v$ are the horizontal and vertical velocity components, respectively. The velocity components are derived from a single stream function $S$:

$$\left.\begin{aligned}&u=\frac{\partial S}{\partial y}\\&v=-\frac{\partial S}{\partial x}\end{aligned}\right\} \quad \cdots\cdots(4)$$

Substituting (3) and (4) into (1) and then cross-differentiating the two equations of (1) with respect to $y$ and $x$, a generalized biharmonic equation in the stream function is obtained:

$$4\frac{\partial^2}{\partial x\partial y}\left(\eta\frac{\partial^2 S}{\partial x\partial y}\right)+\left(\frac{\partial^2}{\partial y^2}-\frac{\partial^2}{\partial x^2}\right)\left\{\eta\left(\frac{\partial^2}{\partial y^2}-\frac{\partial^2}{\partial x^2}\right)S\right\}+\frac{\partial \rho}{\partial x}g=0 \quad \cdots\cdots(5)$$

This is the basic equation to be solved numerically.

As regards the boundary conditions, it is assumed that the two sides of the enclosure are surfaces of free slip, so that both the horizontal velocity and the horizontal derivative of the vertical velocity vanish on the both sides. The top of the enclosure is also assumed to be a surface of free slip, on which both the vertical velocity and the vertical derivative of the horizontal velocity vanish. The bottom of the enclosure may be underlain by a more viscous fluid and, therefore, we assume that it is a surface of no slip, so that all velocity components vanish on the bottom. These boundary conditions are expressed in terms of the stream function $S$, as follows:

$$\left.\begin{aligned}&\text{at the sides} \quad \frac{\partial S}{\partial y}=\frac{\partial^2 S}{\partial x^2}=0\\&\text{at the top} \quad \frac{\partial S}{\partial x}=\frac{\partial^2 S}{\partial y^2}=0\\&\text{at the bottom} \quad \frac{\partial S}{\partial x}=\frac{\partial S}{\partial y}=0\end{aligned}\right\} \quad \cdots\cdots(6)$$

In addition to this, the value of $S$ on all the surfaces of the enclosure should be spe-

cified in order for $S$ to be unique in the enclosure. Here it is assumed that

$$S=0 \quad \cdots\cdots(7)$$

at all the sufaces.

### (3) Method of Solution

The basic equation (5) with the boundary conditions (6) and (7) is numerically solved by the combination of the Successive Over-Relaxation (SOR) method and the Marker and Cell (MAC) method. The procedure of solution is briefly outlined as follows.

Firstly, the enclosure for calculation is divided into $M\times N$ rectangular segments called the control volume, where $M$ and $N$ are the number of control volumes in the $x$ and $y$ directions, respectively. The size of each control volume is $\Delta x$ in the $x$ direction and $\Delta y$ in the $y$ direction.

Secondly, the field variables are placed as shown in **Fig. 2.** The stream function $S_{i,j}$, the density $\rho_{i,j}$ and the viscosity $\eta_{i,j}$ are assigned to a point $P$ centered at the $(i,j)$-th control volume, where $i$ and $j$ are location indices in the $x$ and $y$ directions, respectively. On the other hand, the velocity components, $U_{i,j}$ and $V_{i,j}$, are placed at the points that lie on the surfaces of the control volume. This technique of field variable placement, called the "staggered grid" technique, is needed in order to avoid the introduction of physically unreasonable solutions. An excellent explanation of the technique was given by Patankar[24].

Thirdly, a great number of marker particles are used in order to distinguish the viscous fluids from one another and to introduce a Lagrangian description of the resultant flow. Different fluids are marked by different types of particle. They are uniformly distributed at the initial stage of calculation, with each control volume including $5\times5$ particles (see **Fig. 2**). Thus the total number of the marker particles is equal to $25\times M\times N$. All these particles are moved in accordance with the velocity

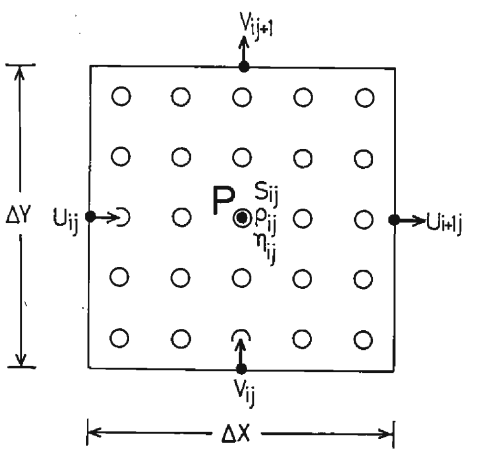


Fig. 2 Placement of field variables in the $(i, j)$-th control volume. Stream function, density and viscosity are placed at the center of the control volume, while velocity components are placed at the points on its surfaces according to the "staggered grid" technique. Open circles indicate the initial distribution of marker particles.

field obtained by the SOR method at each stage of numerical calculation. In this way, the time evolution of fluid flow is represented as a successive change in the distribution of the marker particles.

The mathematical description of the above procedure is given in the **Appendix.** At this point, it is expedint to emphasize that, although the present method is similar to that utilized by Matsumoto and Tomoda[25], there is a difference in the way the "staggered grid" is employed. In their method, the velocity component $U_{i,j}$ was placed at the point that lies on the horizontal surface of the control volume and the component $V_{i,j}$ was placed at the point on the vertical surface. In this paper, as shown in **Fig. 2**, the component $U_{i,j}$ is placed at the point on the vertical surface and the component $V_{i,j}$ at the point on the horizontal surface. This may seem at a first glance to be a minor difference, but it is crucial in obtaining physically reasonable solutions. A numerical test made by the present writer has shown that the method utilized by Matsumoto and Tomoda brings about unreasonable solutions, because the conservation of mass is not fulfilled in the control volume.

### (4) Result

Numerical calculations were performed for the three cases shown in **Fig. 3**. The size of enclosure used for calculation is 460 km in depth. The upper 60 km is initially occupied by the fluid(0) with very low density and viscosity in order that the upper surface of the lithosphere, i.e. the fluid(1), may behave approximately as a free surface. So the features of fluid motions taking place in the lower 400 km is examined. This depth is taken based on the assumption that the increasingly denser mantle located at the depth greater than 400 km would not be significantly affected by the motion under consideration. The width of the enclosure, 1,200 km, is taken as three times the depth. Instead of employing a wider enclosure, which will lead to a highly expensive task, the initial geometrical configuration of the fluids is varied from case to case in order to examine the possible contortion of the resultant flows due to the boundary conditions at the both sides of the enclosure.

As for the physical parameters, in view of the well known fact that a decisive factor controlling the mantle flow is the fluid viscosity, attention is confined mostly to the effect of the viscosity on the features of resultant flows. In particular, taking into account that the lithosphere viscosity so far estimated by several authors ranges from $10^{22}$ to $10^{24}$ poises[26)27)], the three cases shown in the figure are examined. In addition to the above-mentioned lateral density difference, the density inversion between the lithosphere and the asthenosphere is assumed. The values of density shown in the figure are similar to those used by Matsumoto and Tomoda[25].

The enclosure is divided into $60\times23$ control volumes which are square and uniform in size ($\Delta x=\Delta y=20$ km). Thus the total number of marker particles amounts to 34500.

The result is shown in **Figs. 4a-4c**. In these figures, taking full advantage of the MAC method, the time evolution of fluid flow is shown as a gradual change in

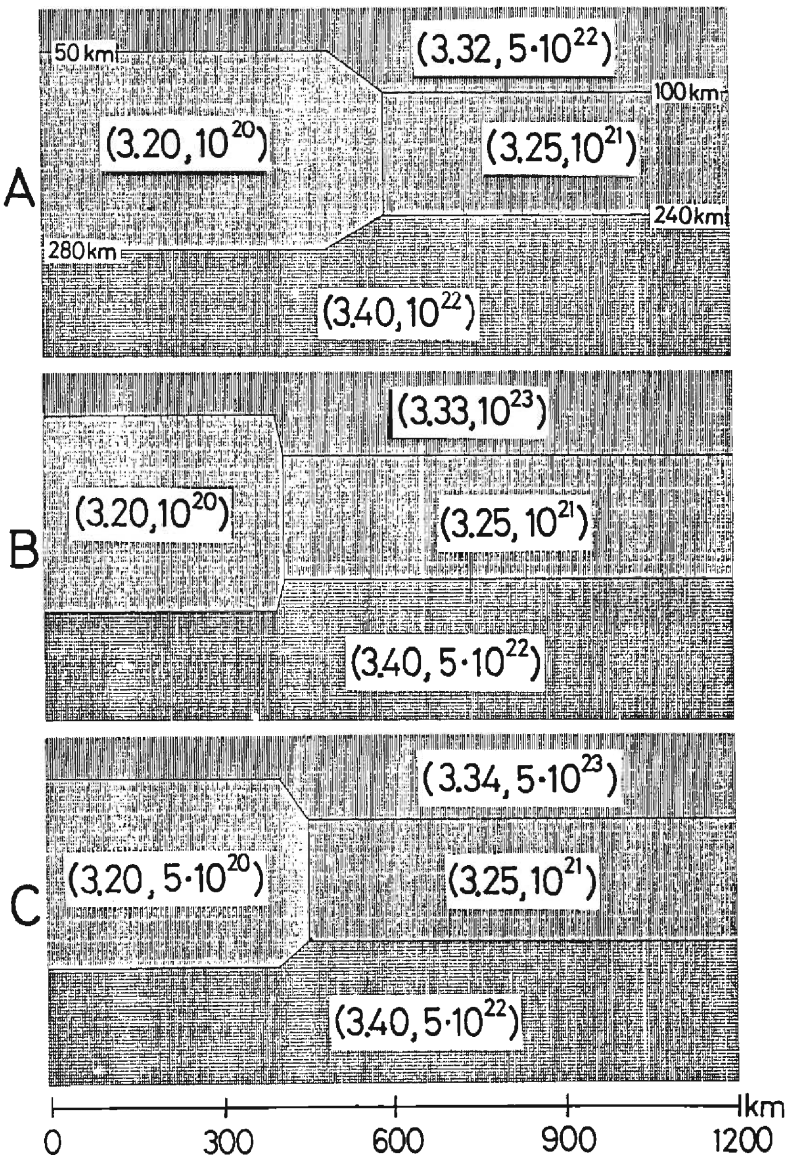


Fig. 3 Geometrical and physical parameters used for calculation. Vertical exaggeration is 3:2. The numerical values in parentheses are density(g/cm$^3$) and viscosity(poises). The 60 km thick horizontal layer of the fluid(0) with $\rho_0 = 0.5$ and $\eta_0 = 10^{-1}$ is not shown.

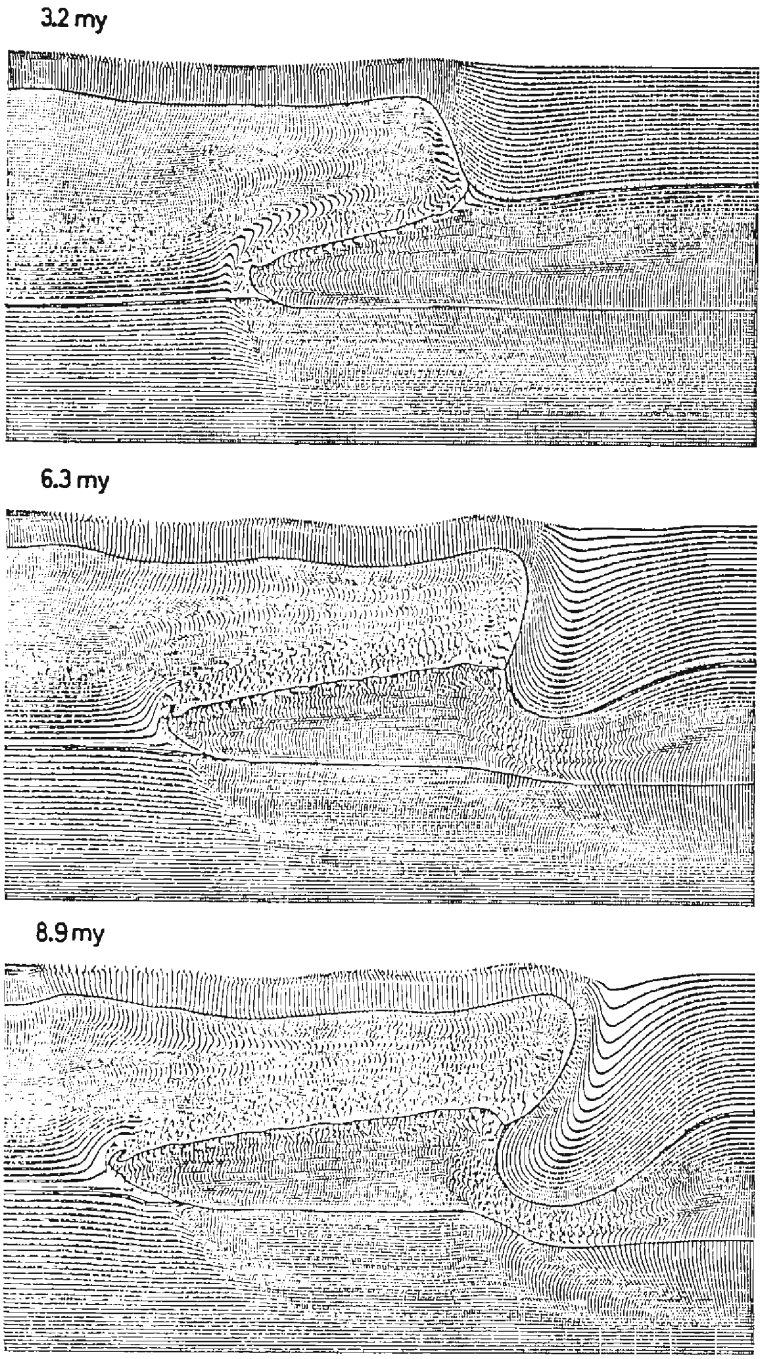


Fig. 4a Time evolution of fluid flow for Case A of Fig. 3.

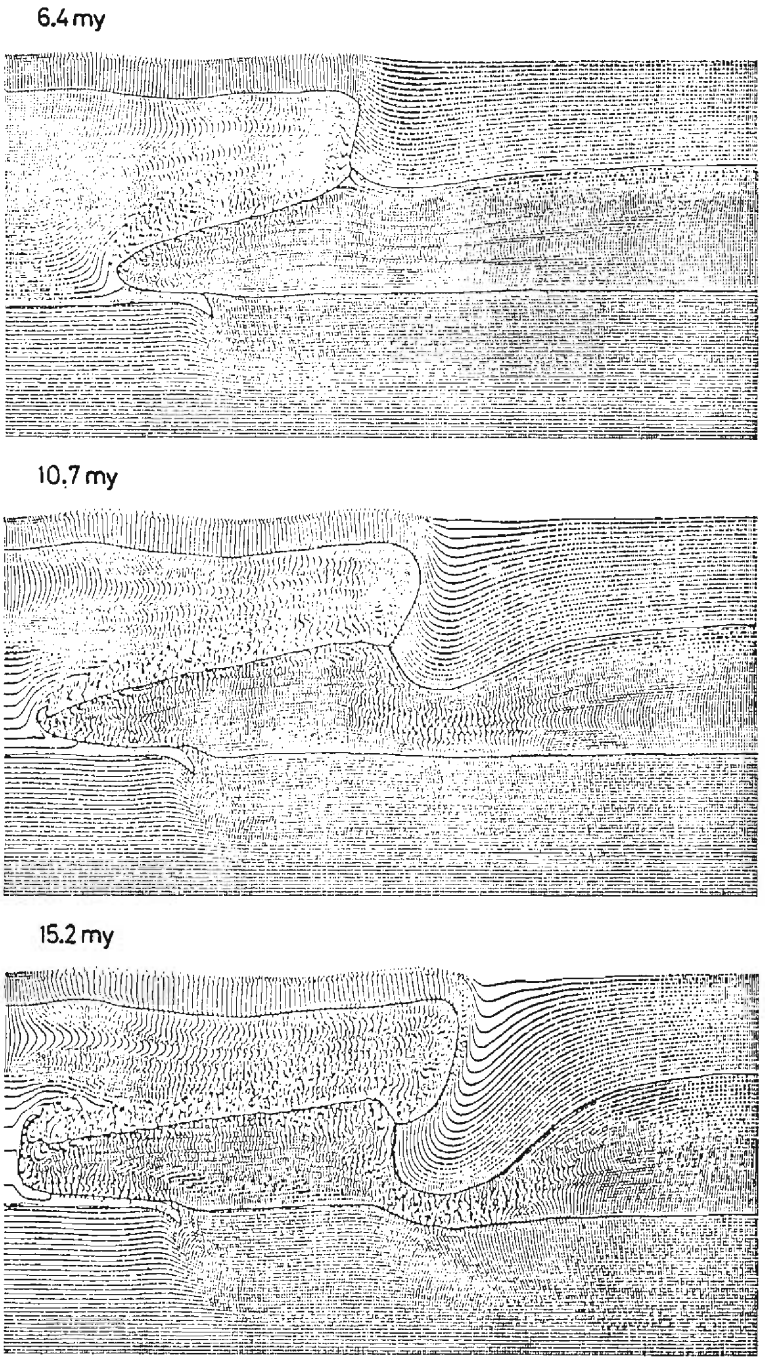


Fig. 4b Time evolution of fluid flow for Case B of Fig. 3.

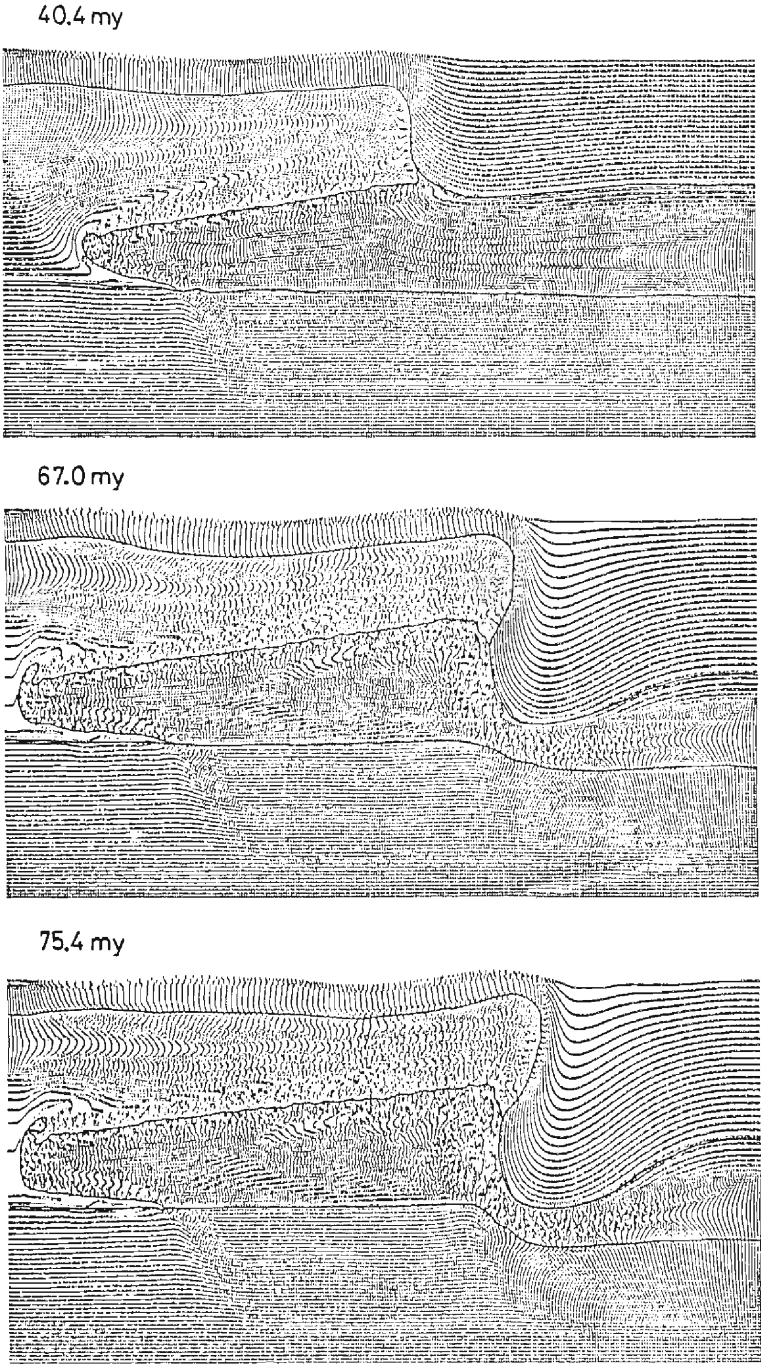


Fig. 4c Time evolution of fluid flow for Case C of Fig. 3.

the distribution of 30,000 marker particles (The rest of the particles marking the fluid (0) is not plotted in order to clearly observe the behavior of the "free" surface of the lithosphere).

A comparison of these figures shows, first of all, that the flow rate depends on the value of the fluid viscosity: the more viscous is the fluid, the more slowly it flows. This is, of course, what can be expected from the equation of motion for viscous fluid. However, it is noteworthy that the fluids are significantly displaced during the lapse of time of several tens million years. This confirms the feasibility of the present model as a working hypothesis in the study of the Cenozoic structural development of the transition zone.

In view of the uncertaities of the physical parameters, it is expedient to examine salient features commonly observed in the figures.

As time progresses, a differential flow grows. The flow rate is highest in the asthenosphere because of its low viscosity. The asthenosphere with lower density flows over the denser asthenosphere and, correspondingly, the latter flows under the former. The flow pattern becomes complicated in the vicinity of contact between the two mutually counter flows. An undulatory motion is observed at the boundary between the asthenosphere and the underlying mesosphere.

What is interersting to note is that some common features can be observed in behavior of the lithosphere.

Firstly, the lithosphere on the left-hand side of the enclosure is subjected to significant extension and, accordingly, the adjacent part of the lithosphere on the right-hand side is thickened and begins to obliquely subside into the asthenosphere. As a result, a wedge-shaped part of the asthenosphere appears between the lithosphere on the left-hand side and the subsiding part of the lithosphere. The oblique subsidence of the lithosphere is caused by the above-mentioned differential flow in the asthenosphere as well as by the density inversion between the lithosphere and the asthenosphere. Its deeper subsidence is restricted by the high density assigned to the mesosphere.

Secondly, notable undulation develops at the "free" surface of the lithosphere which is assumed intially horizontal. The most salient feature is the appearance of a trench-like depression above the most rapidly subsiding part of the lithosphere. In contrast, considerable uplifting of the lithosphere is observed in the adjacently part above the wedge-shaped asthenosphere. As time progresses, this system of uplifting and trench-like depression migrates rightwards, and correspondingly a wide depression appears on the left-hand side of the enclosure. The latter depression is probably associated with the extention of the lithosphere. However, a closer look at the distribution of the marker particles reveals that the lithosphere on the left-hand side is not simply extended, because they are irregularly distributed. This point is examined in the next place with relation to the stress distribution.

In order to get more detailed information, some characteristic features of the state of stress are examined. The normal and the shear stresses are calculated with the use of the stream function (see equations (3)). Some examples of stress distri-

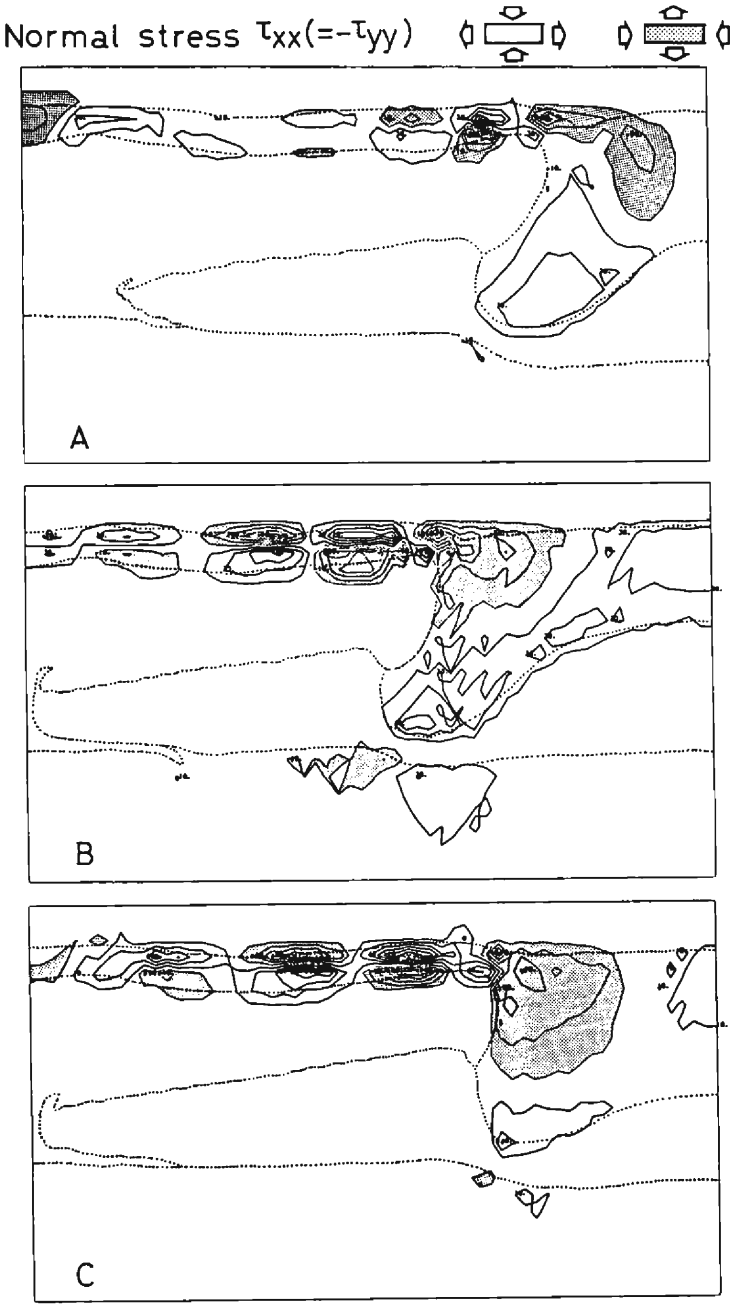


Fig. 5a Examples of the normal stress distribution, A—at 8.9 my for Case A; B—at 15.2 my for Case B; C—at 67.0 my for Case C. Contour interval is $2. \times 10^8$ dyn/cm$^2$. Dotted curves indicate fluid boundaries.

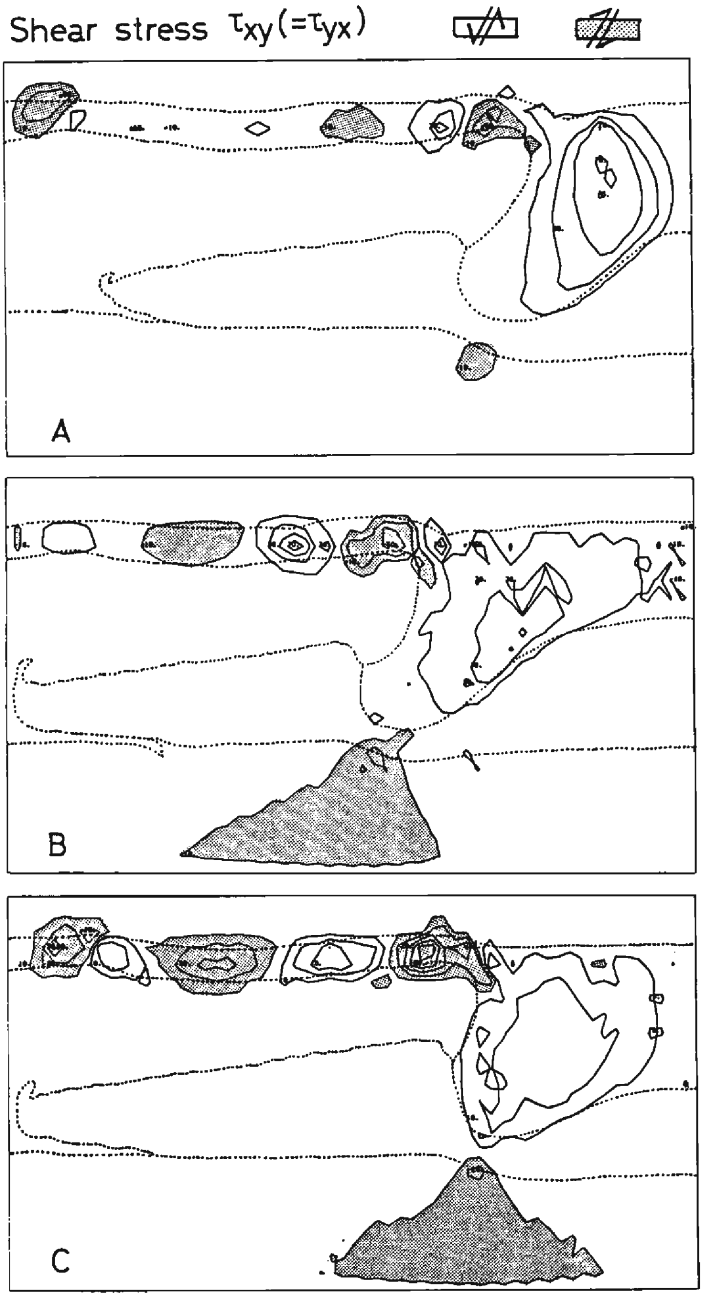


Fig. 5b Examples of the shear stress distribution, A, B, C—same as Fig. 5a.

bution are shown in **Figs. 5a-5b**. In these figures, the stress contours are drawn mostly in the lithosphere, because the stresses are much smaller in the asthenosphere and the mesosphere. This is what can be expected from the low viscosity of the asthenosphere and the low velocity gradint in the mososphere.

It is also expedient to examine common features of the state of stress observed from the figures.

The stress field is relatively simple on the right-hand side of the enclosure. Horizontal compression is characteristic of the upper part of the obliquely subsiding lithosphere. It is large in magnitude near the boundary with the wedge-shaped asthenosphere and, gradually decreasing rightwards, it changes to horizontal tension for Case B and Case C of **Fig. 3**. A similar change is not observed for Case A because of the initial geometrical configuration of fluids. The shear stress is positive(left-lateral) in sign except for the small region beneath the trench-like depression.

In contrast, the stress field on the left-hand side is more complicated. It is characterized by the alternation of tensile and compressional stresses both in the horizontal and vertical directions. Along with the corresponding change in the sign of the shear stress, this feature indicates that the lithosphere is subjected to vertical motion with relatively short wavelength, in addition to the extension mentioned above. This gives a plausible explanation of the irreguar distribution of marker particles observed in **Figs. 4a-4c**. In all probability, the short-wavelength vertical motion is caused by the density inversion between the lithosphere and underlying asthenosphere. In genearal, as demonstrated by Ramberg[28], the velocity and the predominant wavelength of this kind of motion is governed by the ratios of density, viscosity and thickness between the lithosphere and the asthenosphere. Similar vertical motion is insignificant on the right-hand side of the enclousre due to the large thickness of the lithosphere and the small ratio of density.

It is probable that the pattern of the resultant flows is contorted due to the confinement of the fluids within the enclosure for calculation. However, it seems that, as for as the above-mentioned featureses of the flows are concerned, the contortion is not very serious, because they are commonly observed in the three cases to each of which is assigned a different initial configuration of fiuids(see **Fig. 3**). Thus, the generation of fluid flows having the common features is considered to be a natural consequence of the lateral density difference and the density invesion between the lithosphere and the asthenosphere.

## 4. Discussion

In spite of simplicity of the present model, the above result has some significant implications with regard to the Cenozoic structural development of the East Asiatic transition zone.

One of the most interesting features of the calculated result is the development of the contrasting vertical movements of the lithosphere, that is, the notable uplifting above the wedge-shaped asthenosphere and the trench-like depression above the most

rapidly subsiding part of the lithosphere. This feature is in general accord with the geological observation on the extensive development of island arc—trench system in the late Cenozoic, as exemplified by the Island-arc Disturbance which established the present-day structure of the Japanese Islands and vicinity[13]. Thus, it seems possible to infer from the above result that the extensive late-Cenozoic development of island arc—trench system is the surface manifestation of density-driven differential motion in the mantle. As can be seen from the above result, the same differential motion could be also responsible for the appearance of the so-called mantle wedge, that is, the anomalously heated part of the upper mantle situated beneath and beyond the inner side of island arc. Therefore, the above result seems to confirm the actual possibility of the Belousov's supposition[9] that the density-driven differential flow in the mantle played a prominent role in the formation of present-day structure of the island arc—trench system. His diagram is partly cited in **Fig. 6** (Although this diagram is specially concerned with the deep condition from the Southeast Asia to the Mariana Arc, it evidently has general character).

At the same time, however, there is a notable discrepancy between the Belousov's supposition and the above result. No migration of the island arc—trench system is admitted in his diagram, while the calculated result indicates the possibility of some migration of the system. From the viewpoint of fluid mechanics, the migration is considered to be a natural consequence of the density-driven differential flow in the mantle. However, it is not appreciate to conclude from this that the island arc—trench system migrated, because whether it actually migrated or not is to be judged from geological evidence. What can be suggested here is that, as far as the

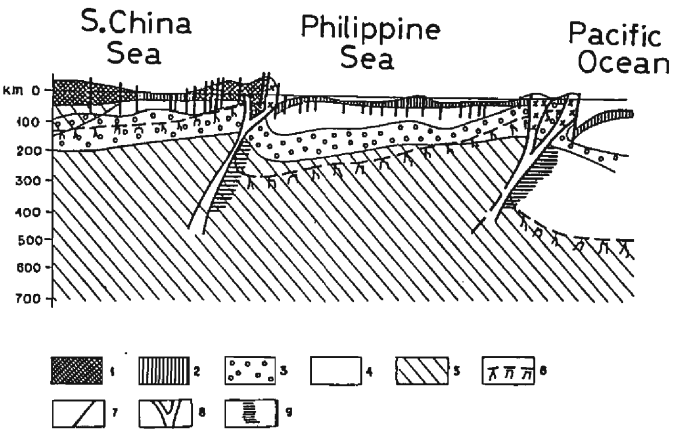


Fig. 6 A part of Beloussov's diagram[9], representing the Late Cenozoic deep condition from the Southeast Asia to the Mariana Arc. 1—continental crust; 2—oceanic crust; 3—asthenosphere; 4—mantle depleted in light and mobile components; 5—undepleted mantle; 6—continental isotherm and uplift of the anomalously heated mantle; 7—faults; 8—Benioff zone; 9—zone of leaching and basification.

mechanical aspect of Beloussov's diagram is concerned, there is no reason to refuse any migration of the Island arc—trench system. In this sense, the above result favors the diagram of Rodnikov and Vadkovsky[8] which, while similar to that of Beloussov, assumes some migration of the system.

Another interesting feature of the calculated result is the complicated state of stress characterizing the lithosphere on the left-hand side of the enclosure. This is probably due to the short-wavelength vertical motion superimposed on the extention of the lithosphere. It is tempting to speculate that the combination of the extention with the short-wavelength vertical motion could create a mechanical condition favorable for the fragmentation of the earth's crust which characterizes marginal basins. In the case of the Japan Sea, the fragmentation is manifested by the alternation of submarine basin with thin crust like the Japan Basin, as well as submarine uplift with thick crust like the Yamato Bank[1].

It is also interesting to note that the horizontal compressional force observed in the upper part of the obliquely subsiding lithosphere is generated without invoking any push from the ocean side. This is the point which was emphasized in the schematic diagram of Nagumo[29], who proposed that the flexure deformation of the lithosphere (in his case, elastic) should be attributed to the forces due to excess mass of crust-mantle mixture which is accumulated beneath the inner side of the Northeast Japan.

Accordingly, as far as the mechanical aspect of process is concerned, the basic features observed from the calculated result offers a possible interpretation of the characteristic features of the Cenozoic structural development of the East Asiatic transition zone.

In this paper, it has been assumed that the mantle located at depths greater than 400 km is too dense (and, probaly, too viscous) to be involved in the motion under consideration. Although further study will be necessary for this point, it is considered at present that a motion involving this part of the mantle has its origin in the deeper part of the earth's interior. One possible mechanism of such motion was offered in one of the previous papers of the present writer[30]. It was suggested that a large-scale differential motion, involving not only the upper mantle but also the upper part of the lower mantle, could be caused by the significant lateral density variation residing in the upper part of lower mantle. It is considered that the tectonic flow investigated in this paper could be superimposed on the large-scale differential motion which flows at a lower rate.

## 5. Summary

(1) An examination of historical sequence of the Cenozoic events in the East Asiatic transition zone made it possible to assume that, at some stage of the Early Cenozoic, there was a significant difference in the temperature of upper mantle between the two sides of the Japanese Islands: higher on the side under the Japan Sea and lower on the side under the Northwestern Pacific.

(2) The mechanical aspect of mantle tectonic flow resulting from this temperature difference was numerically investigated with the use of the SOR method combined with the MAC method to solve the Navier-Stokes equation for variable viscosity problem.

(3) The basic features observed from the calculated result were in general accord with the salient features characterizing the Cenozoic structural development of the East Asiatic transition zone. This lends support to the proposition that density-driven mantle flows played a leading role in the formation of the present-day structure of the transition zone.

## Acknowledgments

The writer expresses his sincere thanks to Dr. Tatsuhiko Wada of Kyoto University for much valuable advice and encouragement. He is grateful to Prof. Yukinori Fujita of Niigata University, Prof. Shozaburo Nagumo of Tokyo University and Dr. Yasumoto Suzuki of the Japan Geological Survey Institute for their continuous encouragement. He is also grateful to Dr. Takeshi Matsumoto of the Japan Marine Science and Technology Center who gave valuable information about the method of calculation.

Numerical calculations were performed on FACOM M 382 and VP 200 at the Data Processing Center of Kyoto University.

## References

1) Vasilkovsky, N.P.: Problems of Origin and Geological History of the Japan Sea, Basic Features of Geological Structure of the Japan Sea Floor, 1978, pp. 215–240 (in Russian).
2) Karig, D.E.: Origin and Development of Marginal Basins in the Western Pacific, J. Geophys. Res., Vol. 76, 1971, pp. 2542–2561.
3) Andrews, D.J. and N.H. Sleep: Numerical Modelling of Tectonic Flow behind Island Arcs, Geophys. J. R. aster. Soc., Vol. 38, 1974, pp. 237–251.
4) Toksöz, M.N. and A.T. Hsui: Numerical Studies of Back-Arc Convection and the Formation of Marginal Basins, Tectonophysics, Vol. 50, 1978, pp. 177–196.
5) Jurdy, D.M. and M. Stefanick: Flow Models for Back-Arc Spreading, Tectonophysics, Vol. 99, 1983, pp. 191–206.
6) Meyerhoff, H.A. and A.A. Meyerhoff: Genesis of Island Arcs, Proceeding of the International Symposium on Geodynamics of South-West Pacific, Paris, 1977, pp. 357–370.
7) Sychev, P.M.: Deep and Superficial Processes in the Northwest of the Pacific Mobile Belt, Nauka, 1979 (in Russian).
8) Rodnikov, A.G. and V.N. Vadkovsky: Mechanism of the Formation of Transition Zone Structure in the Western Pacific Ocean, Volcanology and Seismology, No. 3, 1982, pp. 88–91 (in Russian).
9) Beloussov, V.V.: Certain Problems of the Structure and Evolution of Transition Zones Between Continents and Oceans, Tectonophysics, Vol. 105, 1984, pp. 79–102.
10) Nishimura, K.: On the Character of the Meso-Cainozoic Tectono-Magmatic Activity in East Asia, Bull. Disas. Prev. Res. Inst., Vol. 35, 1985, pp. 41–54.
11) Frolova, T.I. and Yu.I. Konovalov: Volcanism of the Japan Sea as an Indicator of its Formation, Bull. Moscow Univ., Ser. Geology, No. 2, 1985, pp. 54–74 (in Russian).
12) Kaneoka, I.: Constraints on the Time of the Evolution of the Japan Sea Floor Based on Ra-

diometric Ages, J. Geomag. Geoelectr., Vol. 38, No. 5, 1986, pp. 475-485.
13) Fujita, Y.: On the Island-Arc Disturbance, Monograph Assoc. Geol. Collabor. Japan, No. 24, pp. 1-32 (in Japanese).
14) Hilde, T.W.C., S. Uyeda and L. Kroenke: Evolution of the Western Pacific and its Margins, Tectonophysics, Vol. 38, 1977, pp. 145-165.
15) Maruyama, S. and T. Seno: Relative Plate Motions and Orogenesis around the Japanese Islands, Kagaku (Science), Vol. 55, No. 1, 1985, pp. 32-41 (in Japanese).
16) Tatsumi, Y., M. Sakuyama, H. Fukuyama and I. Kushiro: Generation of Arc Basalt Magmas and Thermal Structure of the Mantle Wedge in Subduction Zones, J. Geophy. Res., Vol. 88, 1983, pp. 5815-5825.
17) Honda, S.: Thermal Structure beneath Tohoku, Northeast Japan—A Case Study for Understanding the Detailed Thermal Structure of the Subduction Zone, Tectonophysics, Vol. 112, 1985, pp. 69-102.
18) Miyashiro, A.: Hot Regions and the Origin of Marginal Basins in the Western Pacific, Tectonophysics, Vol. 122, 1986. pp. 195-216.
19) Taylor, B. and G.D. Karner: On the Evolution of Marginal Basins, Rev. Geophys. Space Phys., Vol. 21, 1983, pp. 1727-1741.
20) Shimazu, Y. and Y. Kono: Unsteady Mantle Convection and Tectogenesis, J. Earth Sci., Nagoya Univ., Vol. 12, 1964, pp. 102-115.
21) Rodnikov, A.G.: Island Arcs of the Western Part of the Pacific, Nauka, 1979, 152 pp. (in Russian).
22) Harlow, F.H. and J.E. Welch: Numerical Calculation of Time-Dependent Viscous Incompressible Flow of Fluid with Free Surface, Phys. Fluids, Vol. 8, 1965, pp. 2182-2189.
23) Andrews, D.J.: Numerical Simulation of Sea-Floor Spreading, J. Geophys. Res., Vol. 77, 1972, pp. 6470-6481.
24) Patankar, S.V.: Numerical Heat Transfer and Fluid Flow, Hemisphere Publishing Co., 1980, pp. 118-120.
25) Matsumoto, T. and Y. Tomoda: Numerical Simulation of the Initiation of Subduction at the Fracture Zone, J. Phys. Earth, Vol. 31, 1983, pp. 183-194.
26) Melosh, H.J. and A. Raefsky: The Dynamical Origin of Subduction Zone Topography, Geophys. J. R. aster. Soc., Vol. 60, 1980, pp. 333-354.
27) Hager, B.H., R.J. O'Connell and A. Raefsky: Subduction, Back-Arc Spreading and Global Mantle Flow, Tectonophysics, Vol. 99, 1983, pp. 165-189.
28) Ramberg, H.: Instability of Layered Systems in the Field of Gravity I-II, Phys. Earth Planet. Interiors, Vol. 1, 1968, pp. 427-474.
29) Nagumo, S.: Seismicity and Tectonics of the Island Arc—Trench System in the Northeast Japan, Volcanoes and Tectonosphere, Tokai Univ. Press, 1976, pp. 193-205.
30) Nishimura, K.: A Schematic Model of Development of Active Continental Margins as Inferred form Particular Features of Global-Scale Geoid Undulations, Bull. Disas. Prev. Res. Inst., Vol. 34, 1984, pp. 187-201.
31) Chan, R.K.C. and R.L. Street: A Computer Study of Finite-Amplitude Water Waves, J. Comput. Phys., Vol. 6, 1970, pp. 68-94.

## Appendix

The Mathematical Description of the Method of Solution

Firstly, the values of $\rho_{i,j}$ and $\eta_{i,j}$ are computed by averaging the density and viscosity, respectively, of the fluids inculded in the $(i,j)$-th control volume, as follows:

$$\left.\begin{aligned}\rho_{i,j}&=\sum_{k=1}^{N_{ij}}\rho_k/N_{ij}\\ \eta_{i,j}&=\sum_{k=1}^{N_{ij}}\eta_k/N_{ij}\end{aligned}\right\} \quad \cdots\cdots (A\text{-}1)$$

where $N_{ij}$ is the number of marker particles which come into the $(i, j)$-th control volume, and $\rho_k$ and $\eta_k$ are the density and the viscosity assigned to the $k$-th marker particle.

Secondly, the basic equations((5) to (7) in the text) are transformed into the corresponding finite-difference equations, from which the value of $S_{i,j}$ is obtained by using an over-relaxation technique in conjunction with the Gauss-Seidel point-to-point method of iteration. This technique is generally called the Successive Over-Relaxation(SOR) method and is expressed as follows:

$$S_{i,j}^{NEW}=S_{i,j}^{OLD}+\alpha(S'_{i,j}-S_{i,j}^{OLD}) \quad \cdots\cdots (A\text{-}2)$$

where $S'_{i,j}$ stands for the new value calculated in the current step of iteration, $S_{i,j}^{OLD}$ for the old value from the previous step, $S_{i,j}^{NEW}$ for the value to be used in the next step, and $\alpha$ is a relaxation factor greater than 1 (in this paper, $\alpha=1.40$). The iteration is continued until a sufficient convergence is attained(in our calculation, until the maximum of relative change in $S$ between two successive iterations becomes less than $10^{-4}$). When the iteration converges, the solution $S_{i,j}$ is used for calculation of the velocity field, $U_{i,j}$ and $V_{i,j}$, by employing the following relations:

$$\left.\begin{aligned}U_{i,j}&=(S_{i,j+1}-S_{i,j-1}+S_{i-1,j+1}-S_{i-1,j-1})/4\Delta y\\ V_{i,j}&=(S_{i-1,j}-S_{i+1,j}+S_{i-1,j+1}-S_{i+1,j-1})/4\Delta x\end{aligned}\right\} \quad \cdots\cdots (A\text{-}3)$$

Finally, the marker particles are moved in accordance with the velocity field by using the following relations:

$$\left.\begin{aligned}x_k^{NEW}&=x_k^{OLD}+U_k^{OLD}\times\Delta t\\ y_k^{NEW}&=y_k^{OLD}+V_k^{OLD}\times\Delta t\end{aligned}\right\} \quad \cdots\cdots (A\text{-}4)$$

where $(x_k^{NEW}, y_k^{NEW})$ and $(x_k^{OLD}, y_k^{OLD})$ are the new and old positions of the $k$-th particle, respectively. $U_k^{OLD}$ and $V_k^{OLD}$ are the horizontal and vertical velocities of the $k$-th particle at its old position calculated by the interpolation from the velocity field $U_{i,j}$ and $V_{i,j}$ (Note that the $U_k^{OLD}$ and $V_k^{OLD}$ are the velocities in the Lagrangian description, while the $U_{i,j}$ and $V_{i,j}$ are in the Eularian description). There are two methods of interpolation for the particle velocities, the linear and the second-order interpolations[31]. A preliminary test made by the present writer has shown that no significant difference is found between the calculated results obtained by using

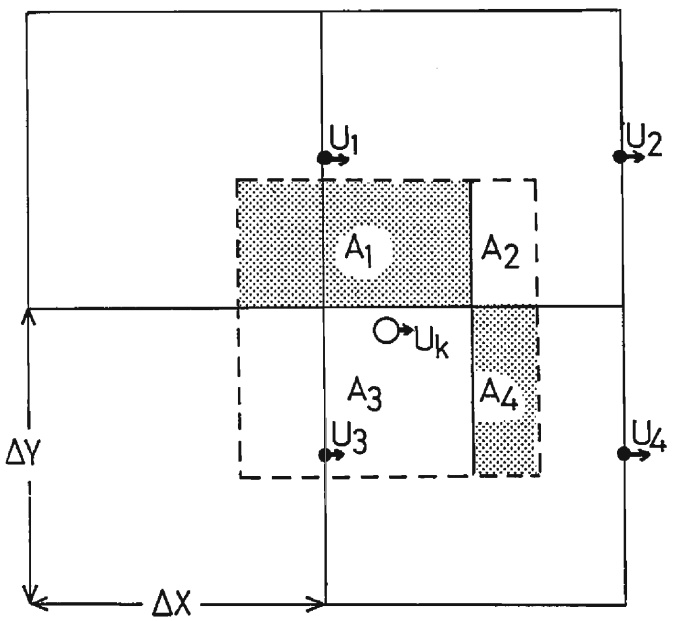


$$U_k = \frac{A_1U_1 + A_2U_2 + A_3U_3 + A_4U_4}{\Delta X \cdot \Delta Y}$$

Fig. A1 Linear interpolation for the horizontal velocity, $U_k$, of the $k$-th marker particle from the velocity field $U_1$ to $U_4$. $A_1$ to $A_4$ indicate the area of rectangular sub-regions. The interpolation for the vertical velocity $V_k$ is performed in a similar way.

the two methods, so the linear interpolation is used (**Fig. A 1**).

In the equations (A-4), $\Delta t$ stands for the time increment of each stage of calculation, which is obtained from the following relation:

$$\Delta t = \beta \frac{\Delta x}{V_{max}} \quad \cdots\cdots (A\text{-}5)$$

where $\beta$ is a constant less than 1 (in this paper, $\beta = 0.75$), and $V_{max}$ is the maximum absolute value of the velocity components $U_{i,j}$ and $V_{i,j}$.